Slim Diffractive Waveguide Glasses for Beaming Displays with Enhanced Head Orientation Tolerance

Yuta Itoh*
The University of Tokyo, Japan

Tomoya Nakamura†
Osaka University, Japan

Yuichi Hiroi‡
Cluster Metaverse Lab

Kaan Aksit§
University College London, United Kingdom

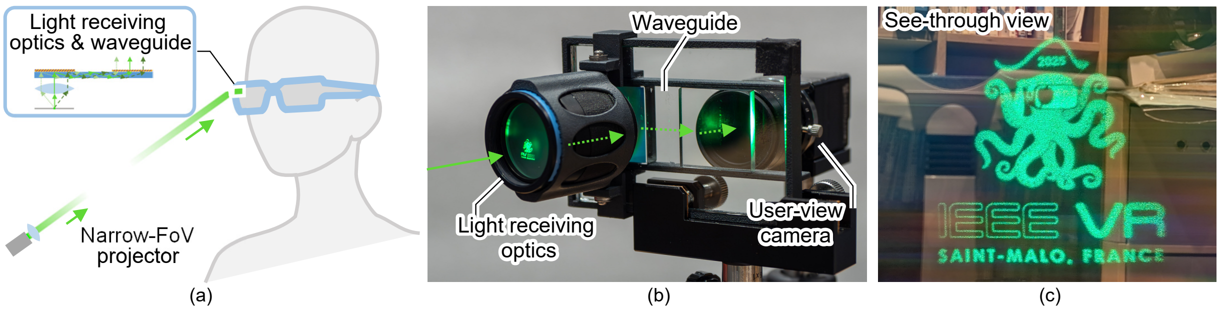

Figure 1: Our waveguide-based light-receiving glasses for Beaming Displays. (a) Conceptual illustration of the beaming display, (b) Our proof-of-concept prototype of passive light-receiving glasses with schematic waveguide path visualization, and (c) a see-through view from the user perspective camera behind the prototype.

Abstract

Augmented Reality (AR) glasses must be slim, lightweight, and energy-efficient to achieve widespread adoption. Beaming Displays present a promising solution by offloading active components, such as the power-supplied light engine, into the surrounding environment while leaving only passive elements, like the eyepiece, in the wearable device. However, existing approaches still struggle to achieve both a slim design and a wide tolerance for projection angles relative to the user's head orientation. In this work, we introduce a design for light-receiving glasses using a diffractive waveguide with in-coupling and out-coupling gratings. Our approach expands the allowable range of incident angles while maintaining a compact, lightweight form factor. We developed a proof-of-concept prototype and demonstrated an incident angle tolerance of approximately 20-30 degrees range, overcoming the previous design of 5 degrees.

Index Terms: Beaming display, Augmented reality, Near-eye display, Waveguide, DOEs.

1 Introduction

Augmented Reality (AR) glasses have the potential to transform digital interactions by seamlessly integrating virtual elements into the physical environment [4]. Despite significant hardware advancements, developing practical and user-friendly AR glasses remains challenging. Key issues include mutually keeping computational power, display brightness, form factor, battery life, and overall weight [10, 16], which collectively hinder the realization of immersive and unobtrusive AR experiences.

*e-mail: yuta.itoh@iii.u-tokyo.ac.jp
†e-mail: nakamura.tomoya.sanken@osaka-u.ac.jp
‡e-mail: y.hiroi@cluster.mu
§e-mail: k.aksit@ucl.ac.uk

Beaming Display (BD) seeks to overcome common limitations of AR displays [9]. Instead of embedding complex electronics and heavy components within the glasses, BD shifts computational and projection tasks to the surrounding environment. In this configuration, steerable projectors track user movements and beam images onto passive, light-receiving glasses [2]. These glasses, free from bulky electronics, relay projected visuals to the user's eyes, potentially enabling lighter and more comfortable AR experiences.

Although existing BD systems address the bulk and weight challenges of traditional AR glasses, they introduce new technical hurdles. These include optimizing latency, coordinating projections from multiple projectors, and improving the size and design of the light-receiving optics (see Sec. 2).

A key challenge unique to BD is ensuring that the glasses can effectively capture and relay projected light over a wide Angle of Incidence (AoI). Unlike conventional AR glasses, BD optics must deliver images to the user's eyes even when the head is not perfectly aligned with the projector's beam. This requirement adds complexity to the optical design, as eyepiece optics must accommodate a wide AoI while maintaining a compact form factor. For example, although the original BD glasses achieved a wide AoI, their birdbath optics were still bulky (Fig. 2(a)).

Recent advancements in BD systems, including the integration of holographic optical elements (HOEs)—a variant of diffractive optical elements (DOEs)—into light-receiving optics, demonstrate potential for creating thinner and lighter AR glasses [1]. However, these designs remain limited by their sensitivity to precise alignment between the projector and the glasses, which affects image visibility. Slight deviations in the AoI can cause the projected light to pass through the HOE lens without forming an image, posing a significant barrier to broader BD system adoption (Fig. 2(b)). *Off-the-shelf HOE-based waveguide systems for AR glasses cannot achieve the necessary AoI, as they are designed for carefully aligned display setups.*

To address these challenges, we developed a light-receiving optic system that combines a diffraction grating-based waveguide with light-receiving screen optics (Fig. 2(c)). Table **??** presents a qualitative comparison of our approach with existing methods. Our main contributions are:

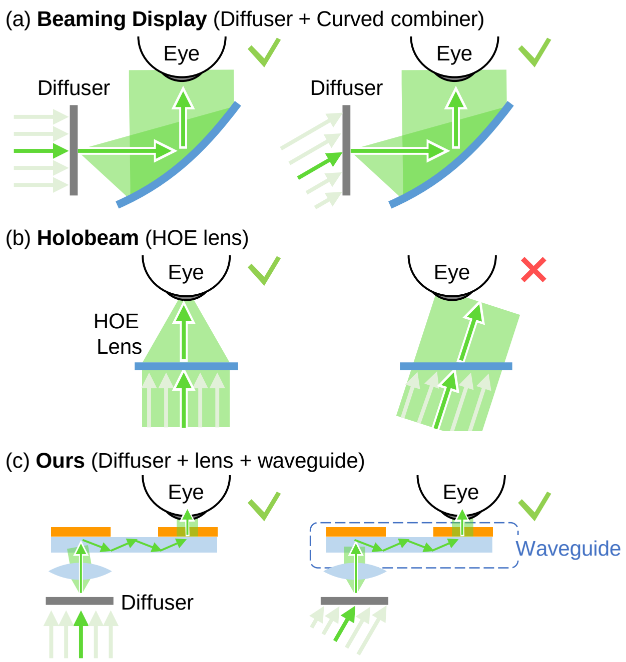

Figure 2: Schematic visualization of the AoI tolerance of existing BD receiving optics. (a) Beaming Display can accept projection from wide AoI, yet the receiving optics are hard to miniaturise [9], (b) HoloBeam uses an HOE lens, which has extremely severe AoI range due to the Bragg condition requirement in its diffractive property [9], and (c) Our design with waveguide.

- **Wide AoI Eyepiece:** We propose a passive light-receiving glasses design featuring a grating-based waveguide for BDs, achieving a wider AoI and supporting slim waveguides with an effective AoI range of approximately 20–30° for horizontal and vertical head orientations.
- **Prototype and Evaluation:** We developed a prototype and demonstrated with a narrow field-of-view (FoV) projector, providing a foundation for further exploration in this research area.

2 Related Work

This section reviews BD and waveguide technologies that underpin our passive optical glasses design.

2.1 Beaming Display Approach

The BD approach offers the potential for addressing feature trade-offs in conventional AR displays. However, current implementations face challenges such as glasses weight [9], display latency [7], and limited scalability of tracking volume [28, 2].

Akşit et al. proposed a holographic lens approach for passive light-receiving glasses, employing an HOE lens to create flat, thin optical glasses [1]. The core concept involves using an HOE lens—a flat, tilted optical element—that directly forms a virtual image at the wearer's viewpoint. They further proposed integrating the HOE lens with a spatial light modulator to enable computational holography for projection. However, the angular selectivity of these holographic lenses necessitates precise alignment between the incident image projection and the lens (Fig. 3(b)). Even a few degrees of angular deviation can lead to a significant reduction in brightness efficiency [31].

2.2 Waveguides for AR Displays

AR displays produce images by directing light from a microdisplay source to the user's eyes [31, 33]. Among various methods for guiding light, waveguide-based approaches have emerged as the dominant solution in the field [17, 33, 20, 5] (Fig. 3(b)). Waveguides offer several advantages, including compact design and the ability to fold light paths, which enable thinner and more flexible devices. Key components of waveguides include light input and output couplers, often implemented using DOEs or metasurfaces that incorporate additional functionality, such as a lens. However, off-the-shelf HOE-based waveguide systems for AR glasses do not necessarily guarantee a large AoI for BD eyeglasses, as they are designed to function with well-aligned display systems [32].

Table 1: A qualitative comparison of the performance of receiving optics in existing beaming-display approaches.

	Beaming Display [9]	HoloeBeam [1]	Ours
Screen optics	Diffuser	None	Diffuser, Lens
Guiding optics	Bird-bath optics with curved beamsplitter	HOE lens	Waveguide with diffractive gratings
Size	Bulky	Thin	Thin
Head orientation	Flexible	Limited (ca. 5°)	Flexible (ca. 20–30°)

DOEs interact with light based on specific wavelengths AoI. Diffractive gratings manipulate light differently depending on its wavelength, while in HOEs, only light of the designed wavelength interacts, and light of other wavelengths passes through unaffected (Fig. 3(a)). This wavelength selectivity makes HOEs ideal for use in see-through optics, such as AR displays, where transparency and image clarity are critical [13]. However, HOEs can be overly selective regarding AoI tolerance, which may restrict the field of view (FoV) in AR displays. In standard AR display designs, the fixed positional relationship between the microdisplay and the waveguide mitigates this issue. In contrast, the beaming display (BD) system does not rely on a fixed configuration, making the selectivity of HOEs a critical factor for head orientation [1, 11] and the achieved image FoV at the user's viewpoint, as observed in our previous HOE-based waveguide system [11]. Diffractive gratings can address this limitation by offering greater AoI tolerance, albeit at the cost of reduced light transmission efficiency.

Metasurfaces utilize subwavelength structures to precisely control light properties, offering greater flexibility compared to traditional optical elements. This flexibility includes the ability to manipulate polarization [27] and compatibility with broader wavelength ranges. These capabilities make metasurfaces a versatile tool in the optical design of AR displays [20, 18]. However, the fabrication of metasurfaces is significantly more complex and resource-intensive than HOEs, requiring access to specialized nanofabrication facilities and advanced techniques, such as electron beam lithography or femtosecond laser nanoprinting. In contrast, HOEs can be produced using readily available photopolymer films and simpler holographic recording processes, making them more practical for widespread applications.

In traditional AR displays, particularly those available commercially, microdisplays are typically placed near the user's eye, often close to the hinge of the glasses. In these designs, light is emitted toward the user from the microdisplay and then guided into the eye via in-couplers positioned accordingly. In contrast, the beaming-display (BD) system assumes that the light originates from the surrounding environment, projecting images from the scene toward the glasses. This arrangement requires the in-coupler to be positioned to face the scene, unlike the conventional waveguide configurations found in standard AR displays (Fig. 3(c)).

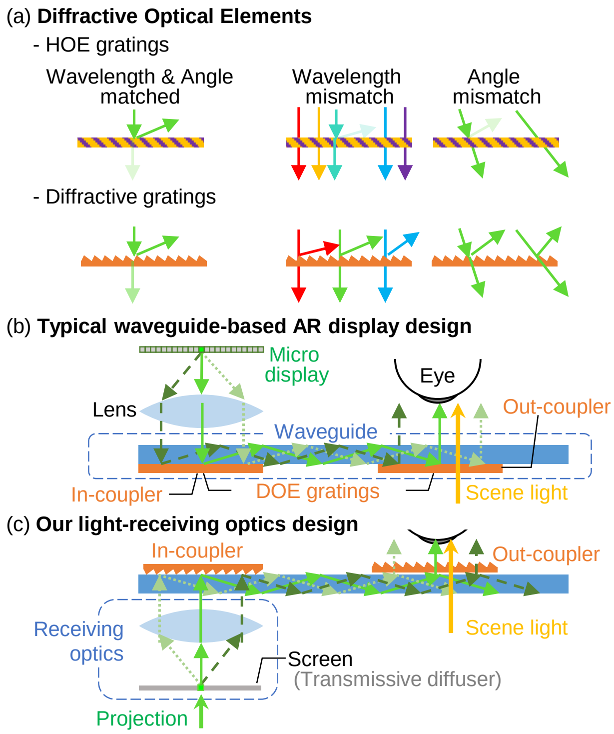

Figure 3: Diffraction-based gratings and waveguides overview. (a) Illustration of the behavior of diffractive optics (gratings) designed to redirect incident light. (b) A simplified, typical waveguide configuration for AR glasses directs light from a face-side microdisplay to the eye. (c) Our Beaming Display approach uses a scene-side screen and DOE couplers to direct incident projection light to the eye.

A similar approach to this opposing coupler layout was proposed by Jang et al. for near-eye holographic AR displays using nano-imprinted surface relief gratings [13]. For our BD system, we have selected HOEs as the preferred coupler technology due to their favorable balance between optical performance and ease of fabrication. Nevertheless, it is important to note that both metasurfaces and DOEs remain viable alternatives for our design, offering unique advantages depending on the specific requirements of the application.

3 Implementations

We overview the optical design and prototype implementation and a brief review of the optical theory of diffractive gratings.

3.1 Diffractive Gratings for Waveguides

Diffraction gratings are optical elements with a periodic structure capable of splitting and directing light into specific directions. In the context of AR displays, they play a crucial role in waveguides by enabling efficient coupling of light into and out of the system. Figure 4 (top) illustrates the geometry and variables associated with diffraction gratings used in AR waveguides.

The interaction of light with a diffraction grating is governed by the grating equation:

$$a\,(\sin\theta_m \pm \sin\theta_i) = m\lambda, \tag{1}$$

where a is the grating period (distance between adjacent grating lines), θ_i and θ_m are the angle of incidence relative to the grating normal and the m-th diffracted order, respectively, and λ is the wavelength of the incident light. The plus sign $(+)$ applies to *reflective gratings*, while the minus sign $(-)$ applies to *transmissive gratings*, indicating the direction of diffracted light.

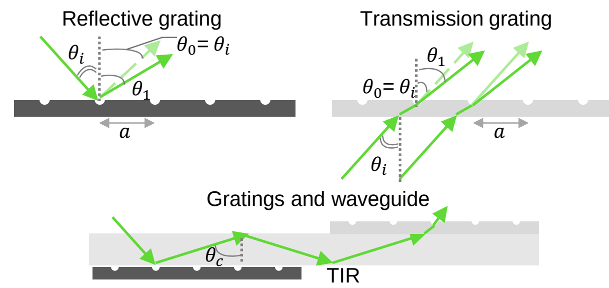

Figure 4: Schematic illustration of the gratings and waveguide with 0-th and 1-st diffracted light. (top) reflective and transmissive grating parameters. (bottom) A waveguide design with TIR. The gratings are required to redirect light rays to achieve the critical angles.

In AR waveguides, two diffraction gratings are typically used as an *in-coupler* and an *out-coupler*. Fig. 4 (bottom) illustrates a configuration featuring a reflective in-coupler and a transmissive out-coupler. Light from the display source enters the waveguide by interacting with the reflective in-coupler grating. This interaction is described as:

$$a\,(\sin\theta_m + \sin\theta_i) = m\lambda. \tag{2}$$

Here, θ_i represents the angle at which the incident light strikes the grating, and θ_m is the angle at which the light is diffracted into the waveguide. The design ensures that the diffracted light enters the waveguide at an angle suitable for propagation via total internal reflection (TIR). TIR occurs when light in a medium with a higher refractive index strikes an interface with a lower refractive index at an angle greater than the critical angle θ_c. The critical angle is defined as:

$$\theta_c = \arcsin\,(n_2/n_1)\,, \tag{3}$$

where n_1 is the refractive index of the waveguide material, and n_2 is that of the surrounding medium (typically air). By ensuring that the in-coupler grating directs light at angles exceeding θ_c, the waveguide confines the light efficiently, enabling it to propagate over long distances with minimal optical losses, which is critical for maintaining image quality in AR displays.

Finally, the light reaches the transmissive out-coupler grating, which diffracts it out of the waveguide toward the user's eye. The grating equation for the out-coupler is:

$$a\,(\sin\theta_m - \sin\theta_i) = m\lambda. \tag{4}$$

where θ_i is the angle at which the guided light strikes the out-coupler grating from within the waveguide, and θ_m is the angle at which the light exits the waveguide. The out-coupler design needs to ensure that the exiting light is directed with the appropriate angle and intensity to provide a clear and bright image for the user.

By utilizing diffraction gratings in this manner, the waveguides can efficiently manage the propagation of light, ensuring that images from the display source are delivered to the user's eye.

3.2 Light-Receiving Glasses

Our light-receiving glasses consist of two main components: screen optics and waveguide optics, as illustrated in Fig. 5(a).

The screen optics feature a diffuser that captures a micro image from the narrow FoV projection and redistributes the light uniformly toward the waveguide by lens optics. The diffuser scatters light across multiple directions, ensuring that the lens optics can capture and direct it effectively to enable a wide AoI. The screen optics include a screen and a lens. For the screen, we used a diffuser (Thorlabs DG10-1500-A, N-BK7, 1500 grit, 1-inch diameter, designed for 350–700 nm) to ensure a uniform distribution of light over the beam AoI. The lens was an achromatic doublet lens

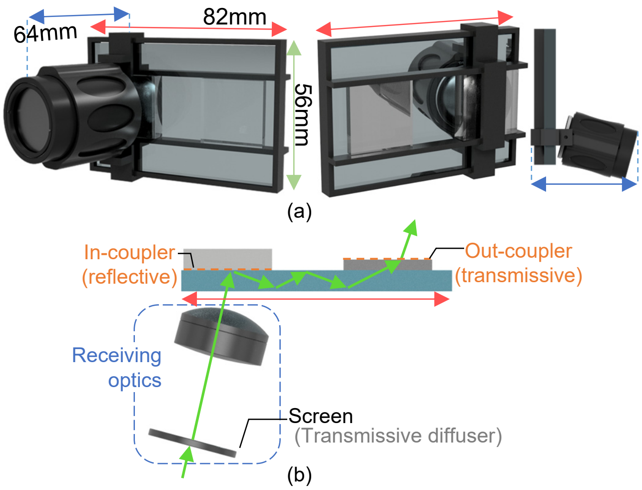

Figure 5: 3D CAD renderings of the designed light-receiving glasses module. (a) Left: A scene-side view. The screen optics receive images from the projector. Right: A face-side view and a top view. (b) A rendering of optical components only with visualization of a schematic optical path of the chief ray.

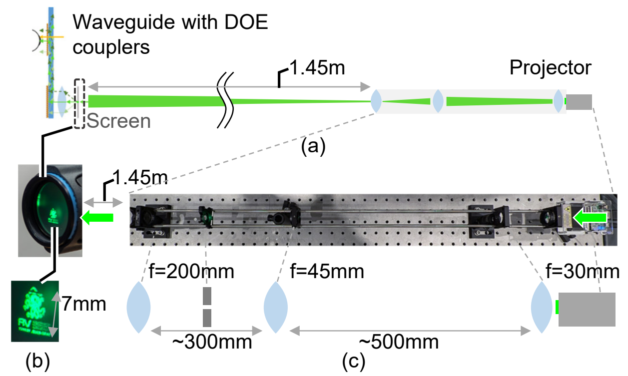

Figure 6: Schematic overview of our system configuration. During experiments, due to limited space, we also placed a mirror between the screen and the projector path to reorient the beam direction and achieve a longer projection distance for demonstration. (a) The system consists of a narrow-FoV projector and light-receiving glasses with a waveguide and diffractive grating couplers. In particular, the in-coupler is placed on the eye-side of the glasses, facing the projector, and relays the projected images into the user's eyes. (b) A sample projection and its schematic of the optical configuration of the narrow-FoV projector. (b) Bird's eye view of the projector and a sample image projected on a white screen about 1.5 meters away.

(Thorlabs AC254-030-A, f = 30 mm, ϕ = 1 inch, a 400–700 nm wavelength range). This lens collimates the projected light onto the waveguide.

The waveguide optics direct light to the user's eyes through TIR. It incorporates two diffractive gratings: an in-coupler and an out-coupler. Positioned on the scene side of the glasses, the in-coupler captures the diffused light from the screen optics and channels it into the waveguide. The light propagates through the substrate via TIR and reaches the out-coupler, located on the eye side of the glasses. The out-coupler then extracts the light and redirects it toward the user's eyes for visualization.

In our design, the waveguide optics are configured with a reflective grating for the in-coupler and a transmissive grating for the out-coupler. The light relaying process begins with the in-coupler receiving light from the screen optics (see Fig. 3(c)). The in-coupler is a Thorlabs GH25-18V holographic reflective grating (1800 grooves per millimeter, 25 × 25 × 6 mm). This reflective grating directs the projected light into the waveguide, ensuring effective guidance through the system. We applied index-matching oil between the grating and the glass substrate. The out-coupler is a Thorlabs GT25-12 transmission grating (1200 grooves per millimeter, 36.9° groove angle, and dimensions of 25 × 25 mm). This grating facilitates light extraction from the waveguide while preserving a see-through view. We also applied index-matching oil here, just as we did with the in-coupler. As the waveguide base, we employed 2 × 3-inch glass plates with a thickness of 2 mm. To improve image separation and reduce crosstalk among different light paths, we stacked three such plates, using index-matching oil between them to minimize reflection losses and optimize light transmission.

To align the waveguide and image-receiving screen optics, we designed and 3D-printed a custom rig to position each optical component accurately. Fig. 5(a, b) presents the 3D CAD model of the rig and a rendering of the optical components with the schematic optical path. The assembled prototype is shown in Fig. 1(b).

4 Evaluation

We evaluate the quality of the see-through images and the AoI capability of our prototypes. In the evaluation setup (Fig. 6), we build a narrow-FoV projector for remote image projection and our light-receiving glasses prototype, respectively.

4.1 Testing Setup with a Narrow-FoV Projector

For our evaluation, we built a projector with a narrow FoV. This setup is designed to project a small image (approx. 7 mm in height) onto the receiving glasses from a distance of about 1.5 m. This contrasts with typical projectors, which generally use a wide FoV.

A steerable projector with a tracking system is ideal for detecting the pose of light-receiving glasses and directing the beam accordingly [7]. However, this study focuses on the waveguide and AoI, and thus dynamic tracking and beam steering were not implemented in the proof-of-concept.

Among the available projection technologies, we chose a laser-scanning projector as the most suitable option. Although digital mirror devices (DMDs) and liquid crystal on silicon (LCoS) projectors are also viable, laser-scanning projectors offer some advantages. First, because diffractive optical elements (DOEs) are wavelength-dependent, a narrow-wavelength light source is needed to maximize resolution and avoid chromatic aberration. Second, using a laser source in two-dimensional spatial modulators (e.g., DMDs or LCoS) causes interference fringes. By contrast, a laser-scanning projector sequentially modulates the beam over time, preventing these interference effects since each pixel is rendered at a different moment. As a future alternative, phase-only spatial light modulators combined with computational holography may be employed [21, 1, 13].

We used an off-the-shelf laser projector (Ultimems HD301D1, 1280 × 980 pixels) and added projection lenses to narrow the FoV, enabling small image projection from a distance (Fig. 6(b, c)). Although cascading long-focal lenses currently result in a longer projector form factor, there is potential for reducing its size, as discussed in Sec. 5.4.

4.2 Evaluation Over Projection AoI

We performed qualitative and quantitative analyses to evaluate the prototype's capability within the projection AoI.

4.2.1 Qualitative Analysis

Figure 7 qualitatively illustrates the system's AoI capability by showing how the image quality changes with varying projection angles. The receiving glasses were mounted on an optical bench

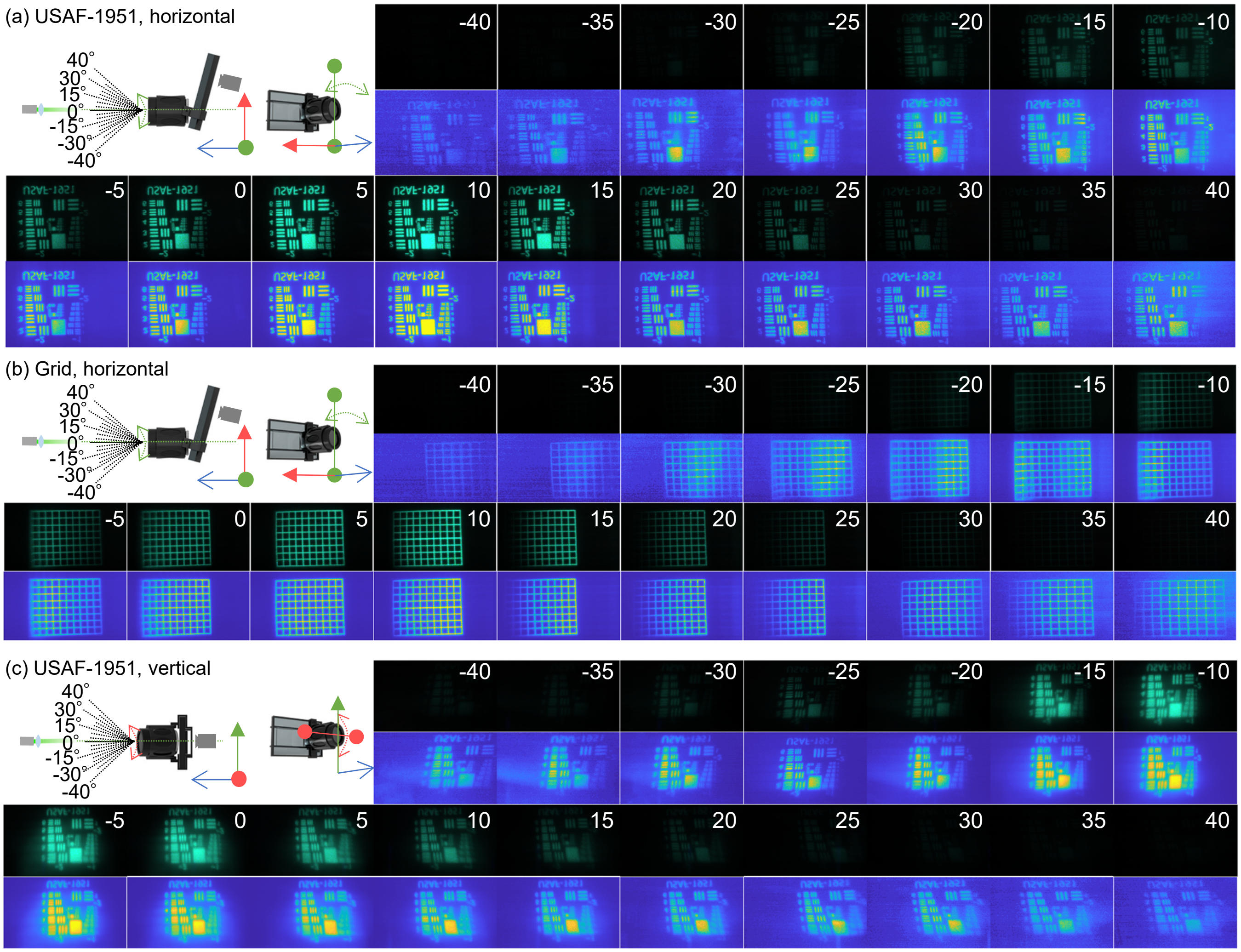

Figure 7: Qualitative display quality evaluation against projection angles. Each image comes with a colormap image to visualize low-intensity images. (a) Horizontal incident angle test with a USAF-1951 chart and (b) with a grid pattern. (c) Vertical incident angle test with a USAF-1951 chart. Brightness and image quality visibly degrade as angles increase.

baseplate and oriented at angles ranging from -40° to 40° in 5° increments, either horizontally or vertically, relative to the projector, while displaying test images.

Image capture was performed using a Ximea MC023CG-SY-UB camera (1936 × 1216 pixels, 1/1.2" diagonal) with a Tamron M118FM25 lens (f = 25 mm, F/1.6), and an exposure time of 16.665 ms (60 Hz). To ensure accurate analysis of the projected image, the room was darkened, and the receiving glasses were covered with black material to eliminate ambient light and block any see-through view.

Figures 7(a) and (b) present the results using a USAF-1951 resolution chart and a grid pattern, respectively, for horizontal orientations of the glasses. Figure 7(c) shows the results with the USAF-1951 chart for vertical orientations. These figures highlight how image quality varies with changes in projection angles.

In all examples, a consistent trend is observed: as the projection angle deviates from the optimal angle for maximum brightness, both brightness and resolution decrease, while geometric distortion and off-focus blur increase. Image distortion can be corrected if the pose of the glasses is known by applying an appropriate homography transform to the input image. The observed blur is likely due to the projection's limited DoF, indicating a need for further improvements in the system's DoF. Qualitatively, the image maintains acceptable quality within an angular range of approximately 20° to 30°. In Figure 7(c), where the vertical projection angle varied, distortion appeared as skew, likely caused by tilting of the receiving screen along both the x and y axes. This distortion can also be corrected through a homography transform.

During the evaluation, the projected images were adjusted to approximately the same position on the screen; however, slight positional shifts were observed, likely due to mechanical alignment limitations. To ensure objective comparison, regions of interest (ROIs) were automatically calculated for each captured image based on the bright areas containing image information. The union ROI of them was subsequently used over the images in the quantitative analysis to provide consistent evaluation metrics.

4.2.2 Quantitative Analysis

Figure 8(a) through (c) presents the quantitative evaluation of the AoI capability. Each figure contains three plots corresponding to the images shown in Figures 7(a) to (c), illustrating Root Mean Square (RMS) contrast, mean intensity, and high-frequency discrete-cosine-transform (DCT) components. For the DCT analysis, the top-left one-fourth of the frequency domain, representing

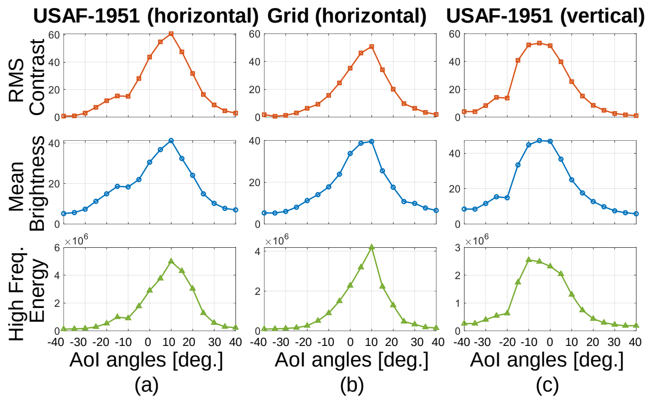

Figure 8: Quantitative analysis of image quality at various projection angles with several image quality metrics. From the top row to the third: RMS contrast, mean brightness, and DCT-based high-frequency metric. The plots illustrate similar performance trends for both horizontal and vertical incident angles.

dominant low-frequency components, was excluded. The remaining high-frequency regions were summed to quantify fine image details.

As shown in Fig. 8(a) and (b), the horizontal AoI evaluation reveals consistent metric peaks at +10°, confirming our qualitative observation that images captured at +10° appear sharpest and brightest. A similar trend is observed in the vertical AoI, with a peak at -10°. Given the distribution shape, if we use a threshold set at 50% of the peak high-frequency energy, the valid AoI angle range is estimated to be approximately 20–30° across all examples, indicating the system's effective angular tolerance.

4.3 User-view Image

We tested our light-receiving glasses prototypes by projecting various digital content. To capture the see-through view, we used a Google Pixel 8 Pro with its 2*times* lens mode. To minimize unintended visual artifacts, the camera's shutter speed was set to 1/30 or 1/60, synchronizing with the laser projector's raster scanning cycle.

Figure 9 (a-c) summarizes our qualitative image evaluation. We tested (a) several static images, including an IEEE VR 2025 logo converted in green with a gamma compensation of 0.3, a USAF-1951 chart, and a grid, (b) 2D animation (Big Back Bunny, copyright Blender foundation), and (c) a 3D CG rendering of a rotating alphabet 'F'. The supplementary video further provides a qualitative visual of the recordings.

5 Discussion and Directions

We discuss the limits and the prospects of our beaming display design with recent advancements in AR optics, as our approach can benefit from these existing optics designed for AR displays.

5.1 Thin Light-receiving Optics

In VR displays, the trend is to reduce the distance from the display panel to the user's eye. Using a Fresnel lens is a common approach in VR headsets to shorten the distance between the microdisplay and the eye while compromising a visual artifact due to its lens structure. Further approaches use pancake optics designs with reflective elements that can even shorten the physical distance between the lens and the waveguide [23, 29].

For such reflective pancake design, an example with a lenslet exists [3]. Further combining reflective liquid crystal HOEs is a promising approach in VR displays [21]. Yet their (circular) polarization dependency may pose challenges as it depends on the projector's polarization, and the beam's polarization angle can be misaligned with the designed angle. We currently use a volume HOE in our design, which is less polarization-dependent and can be used with a wider range of projectors.

As we briefly mentioned in the introduction, a recent design with an opposing layout for a holographic near-eye display can be transferred to our approach [13]. Because we can replace their spatial light modulator part with our light-receiving optics. Multifunctional HOEs, such as integrating lens and grating/diffuser features together, can also reduce the form factor [8, 22].

5.2 Image Quality

The current prototype perceives some visual ghost and vignetting in the peripheral FoV. Despite implementing a reflective diffraction grating as the in-coupler and transmissive diffraction grating as the out-coupler in our waveguide-based AR display, we have observed two primary issues affecting the quality of the see-through image: Limited Field of View (FoV): The peripheral regions of the displayed image appear vignetted, resulting in a restricted FoV. Ghost Images: Duplicate images appear to shift alongside the main image, creating a ghosting effect.

5.2.1 Ghost Image

The ghost images are likely due to the diffraction gratings not achieving 100% diffraction efficiency. When light interacts with the diffraction grating, it splits into two components: the diffracted light and the specularly reflected (non-diffracted) light. The non-diffracted light continues to propagate within the waveguide and can reflect back to the grating. Upon a second interaction with the grating, a portion of this light is diffracted out of the waveguide, resulting in a shifted duplicate of the original image—a ghost image.

This phenomenon occurs because the residual non-diffracted light maintains sufficient intensity to produce visible secondary images upon subsequent diffraction events. The position and intensity of these ghost images depend on the angles of incidence and diffraction, as well as the geometry of the waveguide.

We also note that, unlike commercial waveguides, our custom waveguide had to place separate grating pieces on the glass substrate with index-matching oil. This causes the out-coupler to protrude from the glass substrate plane. Unintended reflections may occur on the sides of the protruding surfaceFig. 5(b). A possible solution is to absorb the non-diffracted light to prevent it from causing ghost images. Blackening the grating grooves could absorb unwanted reflections, but this would eliminate the see-through capability of the display, which is undesirable for AR applications.

Optimizing parameters such as the glass thickness, incident angle, projection image area, and grating area may help reduce ghosting by minimizing the opportunities for non-diffracted light to produce secondary images [34, 24].

A more fundamental solution involves making the diffraction grating polarization-selective. By implementing wave plates on the sides of the glass that are not associated with the gratings, we can design the diffraction gratings to diffract only specific polarization states of light. This method can reduce unwanted reflections and ghost images without compromising transparency [25].

5.2.2 Limited FoV

The limitation in FoV is likely due to the angular dependence of the diffraction efficiency of the gratings. Even with monochromatic light, the efficiency with which a diffraction grating diffracts light varies with the angle of incidence. As the incident angle deviates from the optimal angle for the desired diffraction order (e.g., the +1st order), the constructive interference that maximizes diffraction efficiency diminishes. This results in a decrease in diffracted light intensity at larger incident angles, causing vignetting in the peripheral regions of the image.

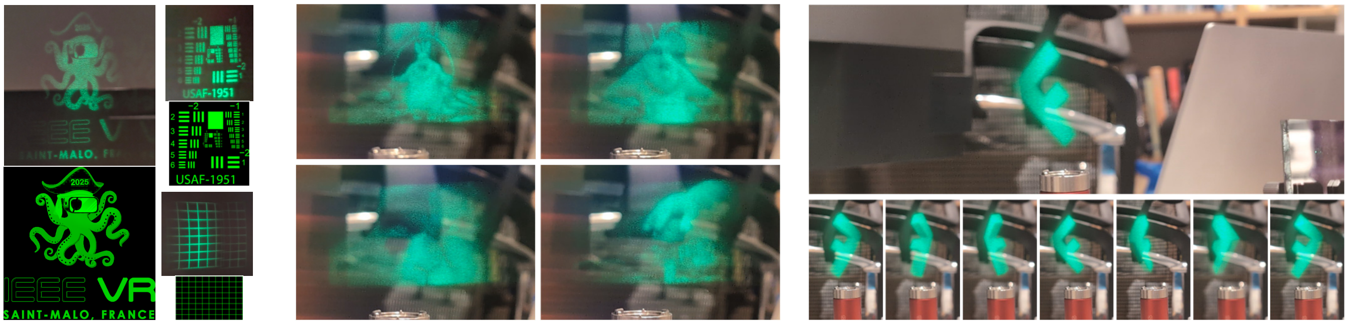

(a) (b) (c)

Figure 9: See-through view samples. The screen AoI was set to 0°. Captures are from (a) static images: a VR2025 logo, USAF-1951 chart, and a grid pattern. (b) 2D animation (Big Back Bunny, © Blender foundation), (c) a 3D CG rendering of a rotating alphabet 'F'.

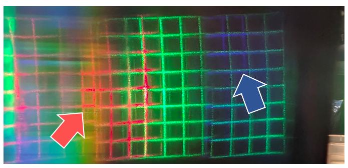

Figure 10: An observation of chromatic aberration in our waveguide system when projected a white grid image. Red (longer than green) and blue (shorter than blue) are shifted in opposing directions.

We considered the possibility that the TIR condition within the waveguide is not satisfied at certain angles, which could lead to light escaping the waveguide and contributing to the limited FoV. However, if TIR failure were the primary cause, we would expect asymmetrical vignetting (i.e., vignetting on only one side of the image), which does not align with our observations.

To address the FoV limitation, we can explore gratings designed to maintain high diffraction efficiency over a wider range of incident angles. This could involve modifying the grating's groove profile or employing advanced grating designs such as blazed or holographic gratings optimized for broader angular performance.

Adjusting the waveguide geometry and optimizing the alignment between the gratings and the projection optics may also help ensure that the incident angles remain within the grating's efficient diffraction range, thereby expanding the effective FoV.

5.3 Full Color Waveguides

Our current prototype with diffractive gratings is optimized for the green channel. Accordingly, the projector only used its green channel during our evaluations. When a full-color image is projected in this setup, it often appears color-split, as shown in Fig. 10.

One common approach for full-color waveguides is stacking multiple ones, each tuned to a specific wavelength (as seen in Magic Leap One/Two from Magic Leap). In parallel, the optics community has explored single-waveguide designs by producing custom waveguides and relay optics [19, 30]. In HOEs, there also exist approaches for full-color HOE, including using multiple HOEs for each color channel [22] or a single HOE with broad bandwidth [26]. More recently, Orion Glasses from Meta Reality Lab employed silicon carbide (SiC) instead of glass for the waveguide base, leveraging SiC's high refractive index to mitigate color splitting.

5.4 Other Topics

Diffuser Improvement The diffuser decides the image quality of the projected images. While we took an off-the-shelf diffuser component, a reflective diffuser or a random micro lens-based diffuser may further improve the resolution. The optical material science community also explores more advanced diffusers with uniform scattering properties with micro/nanoparticles [35].

Narrow-FoV Projection While we located our projector system a meter-half away from the glasses to demonstrate the core concept, greater projection distances may be preferred for indoor or even outdoor applications. The distance range is up to the projection optics design. In spatial AR, for instance, Iuchi et al. integrated a telescope lens with a galvanometer-based scanning laser system, successfully projecting text at distances of up to 200 m [12]. Yet, maintaining a small, high-resolution image over such long distances would be another design challenge. It is worth noting that narrowing the FoV increases the light density over the projection area, potentially making off-the-shelf pico projectors sufficient for the power, provided that suitable projection optics are designed.

Narrow-FoV projection tends to pose depth of field (DoF) challenges, requiring precise screen focus. While laser projectors excel with collimated beams forming sharp spots, our system sacrifices beam collimation for a narrower FoV, resulting in a shallower DoF. A more advanced solution could involve customizing the projector's scanning mirror to retain a narrow FoV with a deeper DoF.

Projection Light Source The choice of the projector's light source presents another design consideration. As discussed, DOEs, including diffractive gratings and HOEs, are wavelength-dependent, meaning that an incompatible wavelength can degrade image quality or render the system non-functional for the designed optics. For this reason, our prototype relied on a laser-scanning projector. While a DMD-based laser projector could be used to increase brightness, it is prone to interference artifacts (i.e., speckle noise), where light from individual pixels interferes with each other. A promising direction for overcoming these limitations is extending the computational holography (CGH) approach using spatial light modulators (SLM), as partially explored in HoloBeam [1]. Recent advancements in VR/AR near-eye displays have successfully combined waveguides with SLMs [13, 15].

Curved Waveguide Typically, waveguides use flat substrates. This limits the design factors and also be incompatible with ordinary prescription eyeglasses. Unlike surface relief gratings, HOEs can be recorded on curved surfaces. Employing curved or even free-form waveguides and optimizing the HOEs accordingly would be an exciting research area to be adapted to our applications as long as we can handle the angular selectivity issue [6, 14].

Tracking and Steering As intended, this work does not incorporate the tracking part of beaming displays, which is yet another essential aspect of the approach. Since our design has wide incident-angle tolerance, it can incorporate the existing approaches. For example, the low-latency dynamic-feedback approach with an IR marker [7] can be applied seamlessly since the DOE couplers do not interfere with the light far outside the designed wavelength.

Stereo Image While this work focuses on a waveguide designed for a single eyepiece, a complete system needs stereo visualization for 3D image generation. One option is to use a dual-projector system that can project stereo images for the left and right eyepieces [2]. Another approach might place a receiving screen at the center of the passive, light-receiving glasses, guiding half of the image to each eyepiece.

6 Conclusion

In this study, we proposed light-receiving glasses with waveguides incorporating diffractive gratings. This design enables thin, passive optical glasses suitable for the beaming display approach, which addresses the trade-offs in AR display design. By optimizing the optical system, we achieved a slim form factor with enhanced AoI tolerance, overcoming the limitations of conventional HOE-based designs. A proof-of-concept prototype was developed and tested using a narrow FoV projector capable of projecting small, high-quality images. The results demonstrate that our design achieves an acceptable lateral AoI range of 20–30°, maintaining virtual image quality. These findings highlight the potential of our approach to advance lightweight and high-performance AR display systems.

Acknowledgments

This work was partially supported by JST ASPIRE Grant Number JPMJAP2327, JST FOREST Grant Number JPMJFR206E and JPMJFR206K, and JSPS KAKENHI Grant Number JP20H05958, JP23H03430 (JP23K28120), and JP23K16920 Japan.

References

[1] K. Akşit and Y. Itoh. Holobeam: Paper-thin near-eye displays. In *Proc. of IEEE VR 2023*, pp. 581–591. IEEE, 2023. 1, 2, 4, 7

[2] H. Aoki, T. Tochimoto, Y. Hiroi, and Y. Itoh. Towards co-operative beaming displays: Dual steering projectors for extended projection volume and head orientation range. *IEEE TVCG*, 2024. 1, 2, 8

[3] K. Bang, Y. Jo, M. Chae, and B. Lee. Lenslet vr: thin, flat and wide-fov virtual reality display using fresnel lens and lenslet array. *IEEE TVCG*, 27(5):2545–2554, 2021. 6

[4] J. Carmigniani, B. Furht, M. Anisetti, P. Ceravolo, E. Damiani, and M. Ivkovic. Augmented reality technologies, systems and applications. *Multimedia tools and applications*, 51:341–377, 2011. 1

[5] Y. Ding, Q. Yang, Y. Li, Z. Yang, Z. Wang, H. Liang, and S.-T. Wu. Waveguide-based augmented reality displays: perspectives and challenges. *eLight*, 3(1):24, 2023. 2

[6] C. T. Draper and P.-A. Blanche. Holographic curved waveguide combiner for hud/ar with 1-d pupil expansion. *Optics Express*, 30(2):2503–2516, 2022. 7

[7] Y. Hiroi, A. Watanabe, Y. Mikawa, and Y. Itoh. Low-latency beaming display: Implementation of wearable, 133μs motion-to-photon latency near-eye display. *IEEE TVCG*, 2023. 2, 4, 7

[8] K. Hong, J. Yeom, C. Jang, J. Hong, and B. Lee. Full-color lens-array holographic optical element for three-dimensional optical see-through augmented reality. *Optics letters*, 39(1):127–130, 2014. 6

[9] Y. Itoh, T. Kaminokado, and K. Akşit. Beaming displays. *IEEE TVCG*, 27(5):2659–2668, 2021. 1, 2

[10] Y. Itoh, T. Langlotz, J. Sutton, and A. Plopski. Towards indistinguishable augmented reality: A survey on optical see-through head-mounted displays. *ACM CSUR*, 54(6):1–36, 2021. 1

[11] Y. Itoh, T. Nakamura, Y. Hiroi, and K. Aksit. Beaming display using thin holographic waveguides for wider head orientation angle range. In *2024 IEEE ISMAR Adjunct*, pp. 475–476. IEEE, 2024. 2

[12] M. Iuchi, Y. Hirohashi, and H. Oku. Proposal for an aerial display using dynamic projection mapping on a distant flying screen. In *IEEE VR 2023*, pp. 603–608. IEEE, 2023. 7

[13] C. Jang, K. Bang, M. Chae, B. Lee, and D. Lanman. Waveguide holography for 3d augmented reality glasses. *Nature Communications*, 15(1):66, 2024. 2, 3, 4, 6, 7

[14] C. Jang, O. Mercier, K. Bang, G. Li, Y. Zhao, and D. Lanman. Design and fabrication of freeform holographic optical elements. *ACM TOG*, 39(6):1–15, 2020. 7

[15] J. Kim, M. Gopakumar, S. Choi, Y. Peng, W. Lopes, and G. Wetzstein. Holographic glasses for virtual reality. In *ACM SIGGRAPH 2022 Conference Proceedings*, pp. 1–9, 2022. 7

[16] G. A. Koulieris, K. Akşit, M. Stengel, R. K. Mantiuk, K. Mania, and C. Richardt. Near-eye display and tracking technologies for virtual and augmented reality. In *Computer Graphics Forum*, vol. 38, pp. 493–519. Wiley Online Library, 2019. 1

[17] B. C. Kress and I. Chatterjee. Waveguide combiners for mixed reality headsets: a nanophotonics design perspective. *Nanophotonics*, 10(1):41–74, 2020. 2

[18] Y. Li, X. Huang, S. Liu, H. Liang, Y. Ling, and Y. Su. Metasurfaces for near-eye display applications. *Opto-Electronic Science*, 2(8):230025–1, 2023. 2

[19] Z. Liu, C. Pan, Y. Pang, and Z. Huang. A full-color near-eye augmented reality display using a tilted waveguide and diffraction gratings. *Optics Communications*, 431:45–50, 2019. 7

[20] Z. Liu, D. Wang, H. Gao, M. Li, H. Zhou, and C. Zhang. Metasurface-enabled augmented reality display: a review. *Advanced Photonics*, 5(3):034001–034001, 2023. 2

[21] A. Maimone and J. Wang. Holographic optics for thin and lightweight virtual reality. *ACM TOG*, 39(4):67–1, 2020. 4, 6

[22] S. Moon, C.-K. Lee, S.-W. Nam, C. Jang, G.-Y. Lee, W. Seo, G. Sung, H.-S. Lee, and B. Lee. Augmented reality near-eye display using pancharatnam-berry phase lenses. *Sci. reports*, 9(1):6616, 2019. 6, 7

[23] B. A. Narasimhan. Ultra-compact pancake optics based on thineyes super-resolution technology for virtual reality headsets. In *Digital Optics for Immersive Displays*, vol. 10676, pp. 359–366. SPIE, 2018. 6

[24] D. Ni, D. Cheng, Y. Liu, X. Wang, C. Yao, T. Yang, C. Chi, and Y. Wang. Uniformity improvement of two-dimensional surface relief grating waveguide display using particle swarm optimization. *Optics Express*, 30(14):24523–24543, 2022. 6

[25] N. Nieuborg, A. Kirk, B. Morlion, H. Thienpont, and I. Veretennicoff. Polarization-selective diffractive optical elements with an index-matching gap material. *Applied optics*, 36(20):4681–4685, 1997. 6

[26] J.-A. Piao, G. Li, M.-L. Piao, and N. Kim. Full color holographic optical element fabrication for waveguide-type head mounted display using photopolymer. *Journal of the Optical Society of Korea*, 17(3):242–248, 2013. 7

[27] J. Tang, S. Wan, Y. Shi, C. Wan, Z. Wang, and Z. Li. Dynamic augmented reality display by layer-folded metasurface via electrical-driven liquid crystal. *Advanced Optical Materials*, 10(12):2200418, 2022. 2

[28] T. Tochimoto, Y. Hiroi, and Y. Itoh. Dual beaming display for extended head orientation and projection volume. In *2023 IEEE ISMAR Adjunct*, pp. 377–378. IEEE, 2023. 2

[29] X. Xia, F. Y. Guan, Y. Cai, and N. Magnenat Thalmann. Challenges and advancements for ar optical see-through near-eye displays: a review. *Frontiers in Virtual Reality*, 3:838237, 2022. 6

[30] J. Xiao, J. Liu, J. Han, and Y. Wang. Design of achromatic surface microstructure for near-eye display with diffractive waveguide. *Optics Communications*, 452:411–416, 2019. 7

[31] J. Xiong, E.-L. Hsiang, Z. He, T. Zhan, and S.-T. Wu. Augmented reality and virtual reality displays: emerging technologies and future perspectives. *Light: Science & Applications*, 10(1):1–30, 2021. 2

[32] J. Xiong, K. Yin, K. Li, and S.-T. Wu. Holographic optical elements for augmented reality: principles, present status, and future perspectives. *Advanced Photonics Research*, 2(1):2000049, 2021. 2

[33] K. Yin, Z. He, J. Xiong, J. Zou, K. Li, and S.-T. Wu. Virtual reality and augmented reality displays: advances and future perspectives. *Journal of Physics: Photonics*, 3(2):022010, 2021. 2

[34] Y. Zhang and F. Fang. Development of planar diffractive waveguides in optical see-through head-mounted displays. *Precision Engineering*, 60:482–496, 2019. 6

[35] L. Zhou, S. Liu, and T. Zhong. A comprehensive review of optical diffusers: progress and prospects. *Nanoscale*, 15(4):1484–1492, 2023. 7